# *Comptes Rendus*

# *Chimie*

Margot Lefèvre, Lielou Lantigner, Laura Andolfo, Corinne Vanucci-Bacqué, Eric Benoist, Charlène Esmieu, Florence Bedos-Belval and Christelle Hureau

**Reduced Schiff-base derivatives to stop reactive oxygen species production by the Cu(Aβ) species: a structure–activity relationship**

Breaking Barriers in Chemical Biology – Toulouse 2022

# Reduced Schiff-base derivatives to stop reactive oxygen species production by the Cu(Aβ) species: a structure–activity relationship

**Margot Lefèvre** [ORCID],*a*, **Lielou Lantigner** *a*, **Laura Andolfo** *a,b*, **Corinne Vanucci-Bacqué** [ORCID],*b*, **Eric Benoist** [ORCID],*b*, **Charlène Esmieu** [ORCID],*a*, **Florence Bedos-Belval** [ORCID],*∗,b* **and Christelle Hureau** [ORCID],*∗,a*

*a* LCC-CNRS, Université de Toulouse, CNRS, Toulouse, France

*b* LSPCMIB, CNRS UMR 5068, Université Toulouse III-Paul Sabatier, 118 route de Narbonne, 31062 Toulouse cedex 9, France

*E-mails:* margot.lefevre@lcc-toulouse.fr (M. Lefèvre), lielou.lantigner@lcc-toulouse.fr (L. Lantigner), laura.andolfo21@gmail.com (L. Andolfo), corinne.bacque@univ-tlse3.fr (C. Vanucci-Bacqué), eric.benoist@univ-tlse3.fr (E. Benoist), charlene.esmieu@lcc-toulouse.fr (C. Esmieu), florence.bedos@univ-tlse3.fr (F. Bedos-Belval), christelle.hureau@lcc-toulouse.fr (C. Hureau)

**Abstract.** Aβ is the peptide involved in Alzheimer's disease. Its binding to the redox copper ions and the subsequent production of reactive oxygen species (ROS) contributing to the overall oxidative stress observed in the disease is among the deleterious effects Aβ may have. Here seven reduced Schiff-base ligands were studied for their ability to stop Cu(Aβ)-induced ROS production. The spectroscopic UV–vis and EPR characterizations of the Cu(II) complexes are reported as well. While all the ligands except one are able to stop Cu(Aβ)-induced ROS, only two maintain this ability in the presence of the endogenous Zn ions, due to kinetic competitiveness.

## 1. Introduction

Alzheimer's disease (AD) is an incapacitating disease that represents the major proportion of dementia cases in the elderly [1,2]. AD is a multifactorial pathology with genetic predispositions and multiple probable causes [3]. Among them, a first hypothesis is known as "the amyloid cascade" [4–6]. It is based on the detection of senile plaques consisting of aggregated amyloid-β (Aβ) peptides, where

Aβ are peptides of approximately 40 amino acid residues in length. Therefore, the process from the monomeric peptides to the amyloid fibrils, so-called self-assembly or aggregation, is regarded as a key element in the development of the disease. Another hypothesis is the "metal hypothesis" [7–9]. It relies on a deregulation of metal ions levels, mainly copper (Cu) and zinc (Zn) ions. It is based on the following facts: (1) metal ions are exchanged with the synaptic cleft where Aβ peptides aggregate, (2) their respective affinities for the Aβ peptides match within their biological concentration, making possible their

interaction with Aβ, (3) aberrant metal levels (up to mM to be compared to μM in the cerebrospinal fluid) are found in the senile plaques. In addition to their likely participation in the modulation of Aβ aggregation [10,11], and because they are redox-active, Cu ions can produce highly deleterious Reactive Oxygen Species (ROS) when bound to the Aβ peptide and thus can participate in the oxidative stress observed in AD [12]. Zn ions are present in much higher quantities than Cu ions in the synaptic cleft and, in contrast to Cu ions, they are redox silent.

Due to its redox ability and participation in oxidative stress, Aβ-bound Cu are thus considered as a therapeutic target of interest among others. We and many other groups have developed many copper-targeting strategies to overrule the deleterious effects of Cu (for recent reviews on that topic, see refs. [13–21] and references therein). Among the various properties, if Cu ions are considered as the target of choice of the intended ligands, they should possess a high Cu over Zn(II) thermodynamic selectivity, much higher than that of Aβ since there are about 10–100 fold more Zn(II) than Cu ions in the synaptic cleft [22,23].

In the present article, we aim to complete seminal works on Schiff base derivatives, used as Cu(II) ligands able to retrieve Cu(II) from Aβ, redox-silence it and be selective enough for Cu(II) versus Zn(II) to maintain such ability in the co-presence of stoichiometric amount of Zn(II). In a seminal paper, Storr and coworkers described the synthesis of glucose derivatives of reduced Schiff base ligands, such as $^G$L$_{Me}$ (Scheme 1), and the thorough characterization of the corresponding Cu(II) complexes [24]. Later on, with the objective of helping *in vitro* characterizations by increasing the solubility of the ligand, the $^s$L$_{Me}$ analogue was reported (Scheme 1). It showed the ability to remove Cu(II) from Aβ, to stop Cu(Aβ)-induced ROS formation, and to restore apo-like aggregation of Cu(Aβ) [25]. Then the $^s$L$_{Me}$ ligand was shown to have an appropriate selectivity to maintain its ability to stop Cu(Aβ)-induced ROS production in the presence of one equivalent of Zn(II) [23]. These ligands have higher affinity and Zn(II) over Cu(II) selectivity than Aβ and hence they maintain the ability to extract Cu from Aβ in the presence of one equiv. of Zn(II). The affinity for a ligand $L$ and a metal ion $M$ is defined as $K_M^L = (LM)/((L)(M))$ while the Cu(II) over Zn(II) selectivity for a ligand $L$ as $S^L = K_{Cu}^L/K_{Zn}^L$.

**Table 1.** Apparent affinity values (for Cu(II) and Zn(II)) at pH 7.1 for the Aβ peptide and the two reference ligands

| $L$ | $\log(K_{Cu}^L)$ | $\log(K_{Zn}^L)$ | $\log(S^L)$ | Ref. |
|---|---|---|---|---|
| Aβ | 9.2 | 5.0 | 4.2 | [26,27] |
| $^G$L$_{Me}$ | 12.1 | 4.6 | 7.5 | [24] |
| $^s$L$_{Me}$ | 13.8 | 6.1 | 7.7 | [25,27] |

The affinity and selectivity values for $^{G/s}$L$_{Me}$ are reported along those for Aβ in Table 1.

Here, we report on the synthesis and characterizations of a series of ligands based on the two $^{G/s}$L$_{Me}$ previously described (Scheme 1). They will be noted $\mathscr{L}$ as a generic term. We aimed to improve the ligand design and several lines were followed: effect of the presence of (i) sulfonato groups on the phenol rings ($^s\mathscr{L}$ versus $\mathscr{L}$), (ii) methyl substituents on the amine functions ($\mathscr{L}_{Me}$ versus $\mathscr{L}$) and (iii) a (±)-trans-1,2-cyclohexyl as bridge ($\mathscr{L}'$ versus $\mathscr{L}$) inspired by previous works on similar scaffolds [28–30]. Rationales for such ligand alterations were (i) to demonstrate that $^s\mathscr{L}$ can be studied *in vitro* while $\mathscr{L}$ could be used for further *in vivo* applications, since the $^s\mathscr{L}$ would not have a correct drug profile, especially to cross the blood–brain barrier, a key step when AD is targeted, (ii) to draw a structure–activity relationship, linking Cu(II) first coordination sites and the arrest of Cu(Aβ)-induced ROS production including in the presence of Zn(II), and (iii) to question kinetic issues beyond the thermodynamic approach mostly described until now.

## 2. Results

### 2.1. *Ligands* $\mathscr{L}$

The synthesis of the ligands has been adapted from literature [31–36] and is described in the Supporting Information.

### 2.2. *Characterizations of Cu($\mathscr{L}$) complexes*

The Cu(II) complexes, formed in situ by the mixture of quasi-stoichiometric ratio between $\mathscr{L}$ and Cu(II) stock solutions (see Figure S1 for the determination of concentration of $\mathscr{L}$) were characterized by UV–vis and EPR spectroscopies. Their signatures are shown
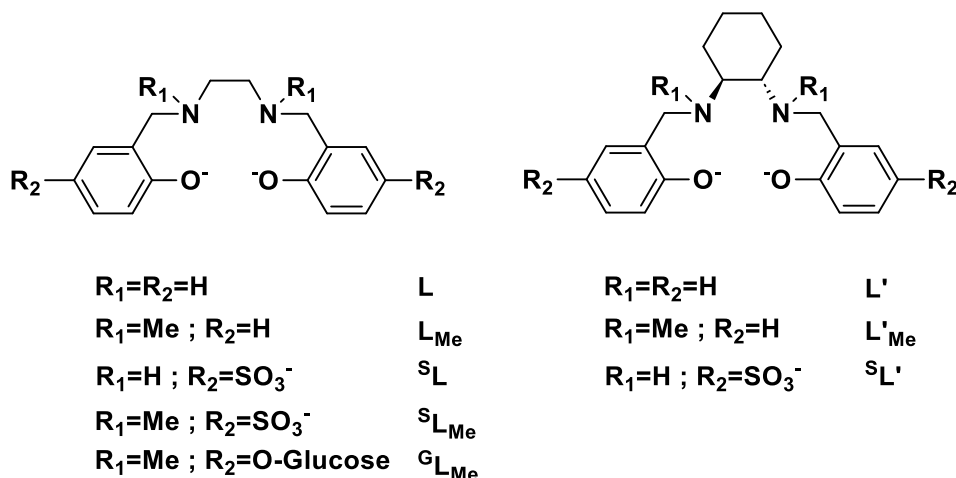
**Scheme 1.** Scheme of the various ligands $\mathscr{L}$ under study. Main variations are methylation of the amine (indicated by the *Me* subscript), sulfonation of the phenol arms (indicated by the *s* superscript), and introduction of a cyclohexyl on the ethylene bridge ($\mathscr{L}'$ series). $\mathscr{L}$ corresponds to the fully deprotonated form of any of the ligands. Charges are omitted for clarity.

**Table 2.** UV–vis and EPR parameters of the Cu($\mathscr{L}$) complexes

| $\mathscr{L}$ | UV–vis | | | | EPR[a] | | |
|---|---|---|---|---|---|---|---|
| | $\lambda_{max}^{d-d}$ (nm) | $\varepsilon^{d-d}$ ($M^{-1} \cdot cm^{-1}$) | $\lambda_{max}^{LMCT}$ (nm) | $\varepsilon^{LMCT}$ ($10^3 \cdot M^{-1} \cdot cm^{-1}$) | $g_{//}$ | $A_{//}$ ($10^{-4} \cdot cm^{-1}$) | $g_{\perp}$ |
| L | **595** | 232 | **382** | 1.24 | $2.23 \pm 0.01$ | $201 \pm 2$ | $2.05 \pm 0.01$ |
| $L_{Me}$ | **603** | 264 | **394** | 1.17 | $2.24 \pm 0.01$ | $198 \pm 2$ | $2.06 \pm 0.01$ |
| $L'$ | **590** | 194 | **382** | 1.18 | $2.23 \pm 0.01$ | $204 \pm 2$ | $2.05 \pm 0.01$ |
| $L'_{Me}$ | **577** | 324 | **398** | 1.30 | $2.23 \pm 0.01$ | $206 \pm 2$ | $2.06 \pm 0.01$ |
| $^{s}L$ | **605** | 251 | **386** | 1.26 | $2.23 \pm 0.01$ | $201 \pm 2$ | $2.05 \pm 0.01$ |
| $^{s}L_{Me}$ | **620** | 254 | **392** | 1.23 | $2.24 \pm 0.01$ | $203 \pm 2$ | $2.06 \pm 0.01$ |
| $^{s}L'$ | **600** | 264 | **382** | 1.35 | $2.23 \pm 0.01$ | $206 \pm 2$ | $2.06 \pm 0.01$ |

[a]The *g* values were calculated using the average position of the second and third hyperfine lines, while the hyperfine coupling values correspond to the field differences between the second and third lines to minimize second-order contributions to hyperfine splittings. $^{65}$Cu isotope was used.

in Figure 1, panels A and B, while the corresponding parameters are listed in Table 2. All the Cu($\mathscr{L}$) complexes show similar features (note that the complexes are neutral with L, $L'$ and $L_{Me}$, $L'_{Me}$ and di-anionic for $^{s}L$, $^{s}L'$ and $^{s}L_{Me}$, but that charges will be omitted for clarity). In UV–vis spectra (Figure 1, panel A), d–d bands and phenolato-to-Cu(II) CT (Charge Transfer) transitions are observed near 600 nm and 380 nm, respectively. Some weak differences are observed according to $\mathscr{L}$. In contrast to the d–d band, the LMCT band is not affected by the presence of sul-

fonato groups on the ligand phenol moiety, whereas the N-methyl group affects it. It should also be noted that the presence of cyclohexyl instead of an ethylene bridge did not affect the LMCT band characteristics. In EPR spectroscopy (Figure 1, panel B), typical spectra of square-planar Cu(II) complexes are obtained, with hyperfine and *g*-value parameters in line with a 2N2O equatorial site, according to the Peisach an Blumberg correlation [37]. Again, some slight differences in the EPR parameters are observed between the various ligands, whereas the presence of two sul-
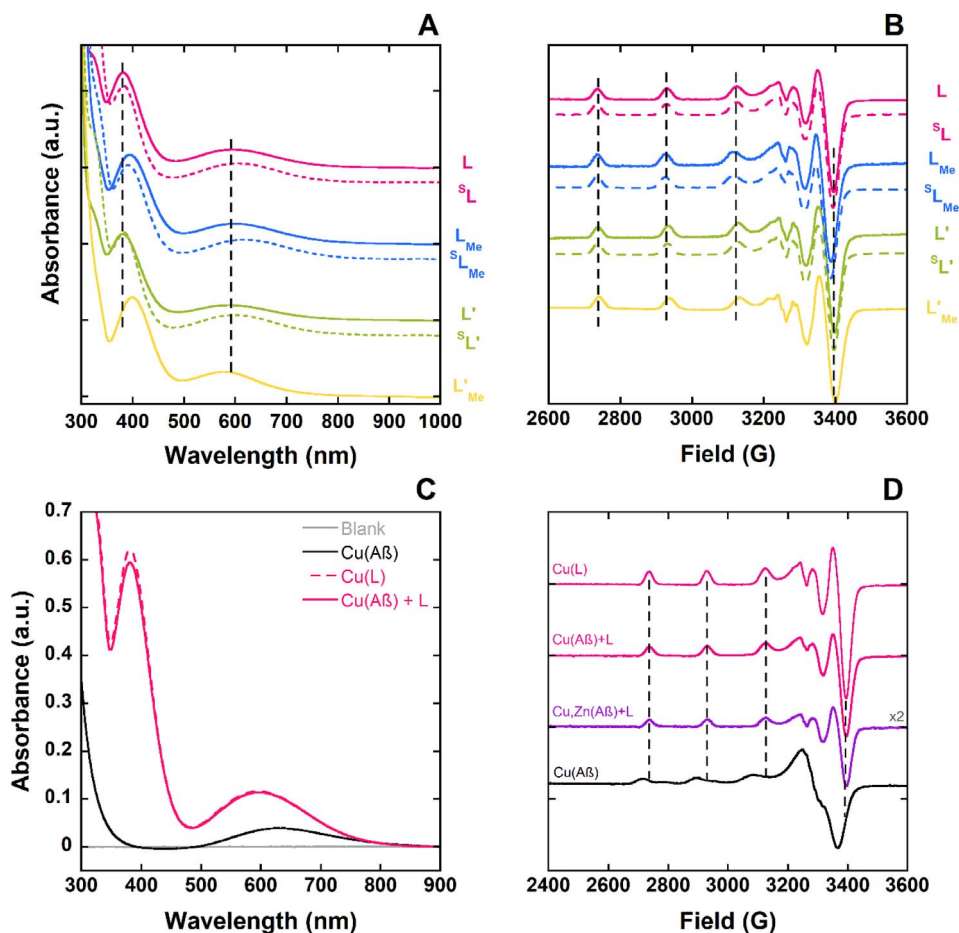
**Figure 1.** UV–vis (Panel A) and EPR (panel B) spectra of the Cu(II)($\mathscr{L}$) complexes. UV–vis (Panel C) and EPR (panel D) spectra of Cu(II) removal by L from Cu(Aβ) and Cu,Zn(Aβ) respectively. Experimental conditions: panels A and C: $[Cu^{II}]$ = 500 μM, $[L]$ = $[Aβ]$ = $[Zn^{II}]$ = 500 μM, [HEPES] = 100 mM, pH 7.4, $T$ = 25 °C; panel B: $[^{65}Cu^{II}]$ = 480 μM, [L, Aβ] = 500 μM; and panel D: $[^{65}Cu^{II}]$ = 480 μM, [L, Aβ] = 500 μM or $[^{65}Cu^{II}]$ = [Zn] = 190 μM, [L, Aβ] = 200 μM; panels B and D: [HEPES] = 50 mM, pH 7.4, 10% of glycerol as cryoprotectant, $T$ = 120 K, ν ≈ 9.5 GHz, mod. ampl. = 5 G, microwave power: 5 mW. In panel D, EPR data corresponding to Cu,Zn(Aβ) + L have been multiplied by 2 in order to account for the 2.5-fold lower concentration used.

fonato groups on the ligands has virtually no impact on the Cu($\mathscr{L}$) EPR signatures. Again, as for UV–vis spectra, methylation of the secondary amine leads to the most significant difference with a decrease in the hyperfine coupling ($A_{//}$) values and an increase in the $g_{//}$ values, while grafting of the cyclohexyl on the ethylene diamine bridge has the opposite effect.

In brief, the spectroscopic characterizations indicate that the first coordination sphere of the complexes are identical in buffered solution, but

that some minor second sphere structural changes occur.

### 2.3. *Cu(II) removal from Cu(Aβ)*

Next, we performed competition experiments, monitored by UV–vis and EPR spectroscopies (Figure 1, panels C and D in case of ligand L and Figures S2 and S3 for the other ligands), to check that the ligands $\mathscr{L}$ were able to remove Cu(II) from Cu(Aβ) including in

the presence of Zn. In other words, we check that $\mathscr{L}$ have higher Cu(II) affinity and Cu(II) over Zn(II) selectivity than Aβ. The spectroscopic signatures of Cu($\mathscr{L}$) were recovered during the competition experiments (Cu(Aβ) + $\mathscr{L}$ or Cu,Zn(Aβ) + $\mathscr{L}$). Thus all the ligands $\mathscr{L}$ are efficient in retrieving Cu from Cu(Aβ) regardless of the presence of one equiv. of Zn(II). Hence, the thermodynamic parameters of $\mathscr{L}$ are suitable for performing Cu(II) removal from Aβ including in the presence of one equiv. of Zn(II). However, during the course of the competition experiment, we noticed that the thermodynamic equilibrium is reached more slowly in the case of the ligand $L'_{Me}$ (about 30 min versus less than 5 min for the others ligands, Figure S4).

## 2.4. *Effect of ligands $\mathscr{L}$ on Cu(Aβ)-induced ROS production*

Finally, Cu(Aβ)-induced ROS formation was evaluated using a very suitable and straightforward experiment, namely the ascorbate (Asc) consumption assay. This is an appropriate method to monitor ROS formation. Briefly, it consists in measuring the absorption of Asc (at 265 nm, $\varepsilon = 14{,}500\,\mathrm{M^{-1}\cdot cm^{-1}}$) that is the reductant fueling the incomplete reduction of $O_2$ to $O_2^{\circ-}$, $H_2O_2$ and $HO^\circ$ [21], and that does not absorb once oxidized. It has been previously shown that Cu and Cu(Aβ)-induced Asc consumption mirrors the formation of $H_2O_2$ and $HO^\circ$ [38,39]. A ligand will be efficient in stopping Asc consumption if it can bind Cu(II) or remove it from Aβ, and then form a Cu(II) complex resistant to reduction by Asc, eventually interrupting the redox cycle of Cu and thus the production of ROS.

With Asc consumption assays, two distinct experiments can be performed, either by incubating the various chemical partners at play and then triggering the reaction by addition of Asc (named "experiments A", Figure S5 and Figure 2, panel D), or by adding ligand $\mathscr{L}$ during Cu(Aβ)-induced Asc consumption (named "experiments B", Figure 2, panels A to C). In experiments A, if the incubation time is long enough, the results indicate the ability of $\mathscr{L}$ to remove Cu from Cu(Aβ) including in the presence of increasing stoichiometry of Zn(II), thus documenting the thermodynamics of the reaction of Cu(II) extraction out

of Aβ. This is a very straightforward way to evaluate whether the selectivity of a ligand *L* is appropriate [22,23]. More specifically, such a method is more suited to screen between various ligands than the individual determination of Cu(*L*) and Zn(*L*) formation that would also release the selectivity of the *L* (see introduction). In experiments B, additional kinetic parameters are involved (Scheme 2A) [40–43]. Indeed, during Asc consumption, Cu oscillates between the +I and +II redox states. To be efficient, the tested ligand thus has to be faster in removing Cu(II) from Aβ than the reduction of Cu(II)(Aβ) to Cu(I)(Aβ) by Asc. In the $\mathscr{L}$ series, we wanted to decipher the importance of Zn stoichiometry in both the thermodynamics (experiments "A") and kinetics (experiments "B") of Cu(II) removal. In the following, all the experiments were performed with 10 μM of Cu(II) ions, 1.2 equiv. of Aβ and/or $\mathscr{L}$, and 0, 1 or 10 equiv. of Zn(II). Note that for practical reasons, the experiments are run with a slight excess of Aβ and/or $\mathscr{L}$ to avoid any possibility of unbound Cu(II) ions and/or Aβ-bound Cu(II) complexes, respectively. Indeed, this would dramatically change the rate of Asc. consumption.

In the absence of Zn and after short incubation (300 s) (Figure S5, panel A), all the ligands except $L'_{Me}$ are able to stop Cu(Aβ) induced Asc consumption. After a longer incubation time (>18 h), $L'_{Me}$ becomes efficient (Figure S6). This indicates that Cu(II) removal from Aβ by $L'_{Me}$ is slower than that with the other $\mathscr{L}$ ligands, but thermodynamically possible, in line with the competition experiments previously described. In addition to showing that all the ligands are able to extract Cu(II) from Aβ, these experiments confirm that all the Cu($\mathscr{L}$) complexes formed are resistant to reduction by ascorbate. In line with these first results, all the ligands, except $L'_{Me}$ and to a lesser extent $L'$ and $L_{Me}$, are able to stop Cu(Aβ)-induced Asc consumption when added during the course of the experiments (Figure 2, panel A).

## 2.5. *Effect of ligands $\mathscr{L}$ on the Cu(Aβ)-induced ROS production in the presence of Zn(II)*

In the presence of Zn, the differences between the various ligands appear more clearly. This may be due to the additional competition reaction between Cu(II) or Zn(II) removal from Cu,Zn(Aβ) (Scheme 2, panel B). With a short incubation (300 s) (Figure S5,
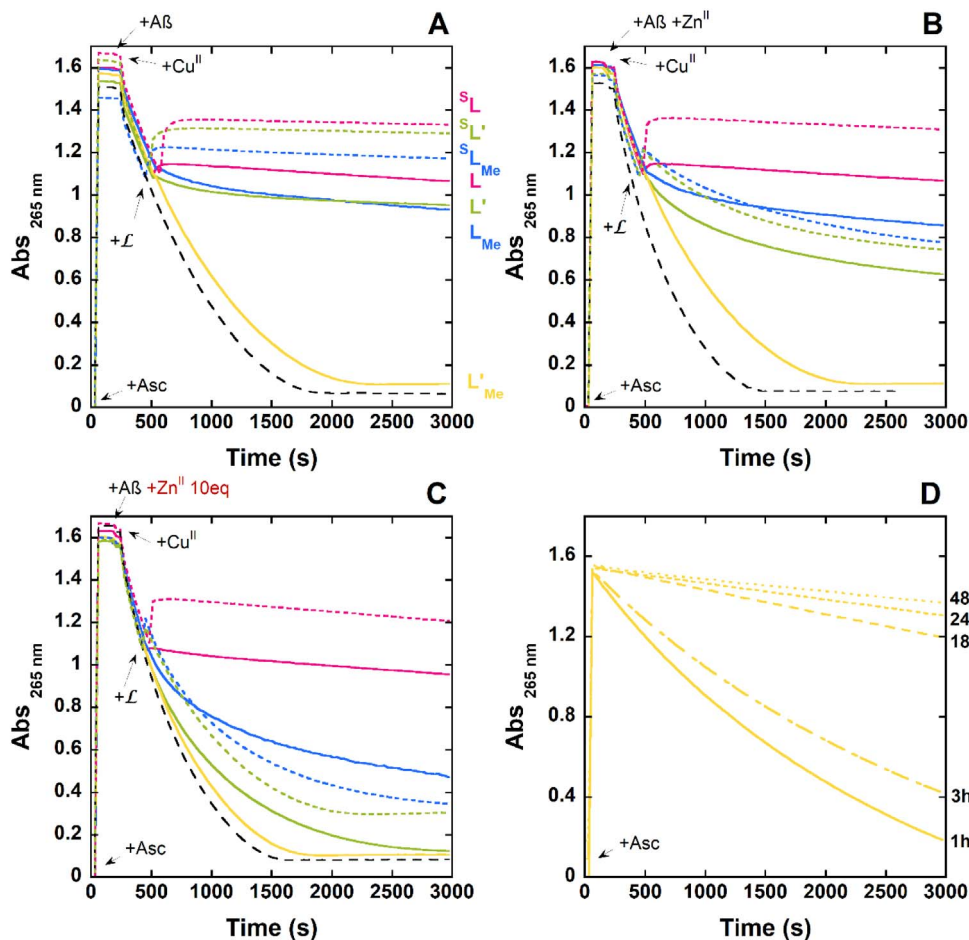
**Figure 2.** Ascorbate consumption is followed at 265 nm (with a baseline subtraction at 800 nm) induced by Cu(Aβ). Panels A to C: starting from a Cu(I)/Cu(II) mixture and in the presence of increasing Zn(II) stoichiometry. $[\mathcal{L}]$ = [Aβ] = 12 µM, $[Zn^{II}]$ = 0, 12 and 120 µM, $[Cu^{II}]$ = 10 µM, [Asc] = 100 µM, [HEPES] = 100 mM, pH 7.4, $T$ = 25 °C. Panel D: starting from Cu(II) and after increasing incubation times from 1 to 48 hours. $[L'_{Me}]$ = [Aβ] = 12 µM, [Zn] = 120 µM, $[Cu^{II}]$ = 10 µM, [Asc] = 100 µM, [HEPES] = 100 mM, pH 7.4, $T$ = 25 °C. The arrows indicate the time at which the different components are added into the cuvette.

panel B) or when the ligand is added during Cu(Aβ)-induced Asc consumption (Figure 2, panel B), the trends are the same. The "efficiency trend" (i.e. the ability of the ligand to stop Cu(Aβ)-induced Asc consumption in the presence of Zn) is as follows: L ~ $^{s}$L > $L_{Me}$ ~ $^{s}L_{Me} \gtrsim {}^{s}L' \gtrsim L' \gg L'_{Me}$. With higher stoichiometry of Zn(II) (10 equiv.), the differences are more obvious and only the L and $^{s}$L ligands maintain their ability to stop Cu(Aβ)-induced Asc consumption (Figure 2, panel C).

Hence, it appears here that Zn(II) induces a change in the ability of the ligands $\mathcal{L}$ to stop Cu(Aβ)-induced ROS production and that this effect is dependent on the ligands $\mathcal{L}$, with a dependence that is more clearly revealed in the presence of 10 equiv. of Zn(II). Two explanations can be proposed (i): when increasing the ratio of Zn(II), the thermodynamic equilibria at play change and the ligand becomes thermodynamically unable to remove Cu(II) from Aβ, or (ii) Zn(II) has a kinetic impact on Cu extraction from Aβ. This kinetic effect would be due to the faster formation of the Zn($\mathcal{L}$) complexes that have
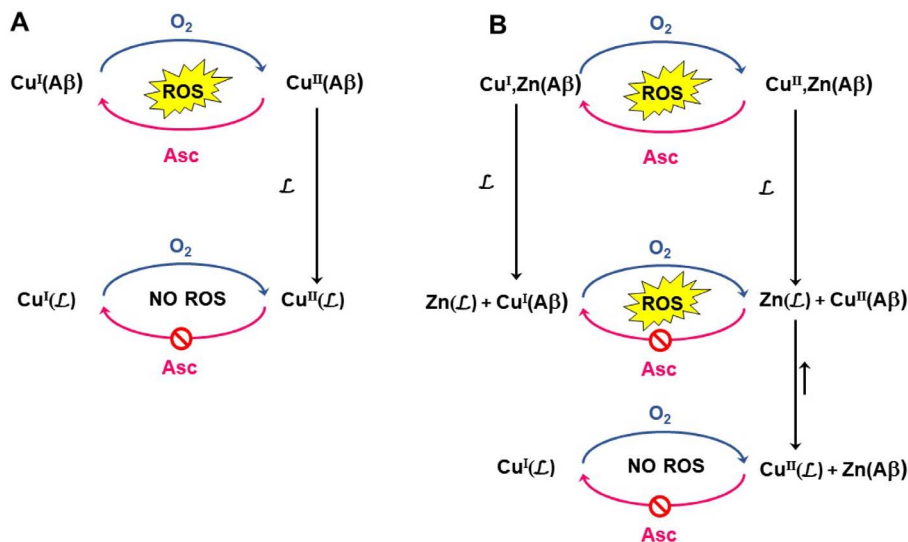
**Scheme 2.** Mechanisms of arrest of Cu(Aβ)-induced ROS production by a Cu(II)-targeting ligand $\mathscr{L}$, in the absence (Panel A) and presence of Zn (panel B). In the absence of Zn(II), the reaction of Cu(II) extraction from Aβ is in competition with Cu(II)(Aβ) reduction by Asc. In the presence of Zn(II), an additional competition reaction occurs due to the possible formation of Zn($\mathscr{L}$) that will retard the formation of Cu($\mathscr{L}$).

further to swap their metallic center with Cu(Aβ) (Scheme 2, panel B). To discriminate between these two hypotheses, we also performed experiments A with a longer pre-incubation time of Cu(Aβ) + $\mathscr{L}$ in the presence of 10 of equiv. Zn(II). Several incubation times were tested: 1, 3, 18, 24, and 48 h (Figure 2, panel D and Figure S7). The results obtained show that with a sufficient incubation time, all the ligands prevent Cu(Aβ)-induced ROS production and thus that the overall effect of Zn(II) is kinetic. For all ligands, except $L'_{Me}$ which requires at least 24 h of incubation, (Figure 2D), 1 h of incubation is sufficient to prevent Asc consumption (Figure S7).

## 3. Discussion

The various results obtained with the ligands $\mathscr{L}$, are compiled in Figure 3, where the rates of ascorbate consumption are reported.

### 3.1. *Effect of p-sulfonation on phenol rings*

The sulfonated version of three ligands were tested. Sulfonation has no significant effect on the properties of the parent ligand regarding Cu(Aβ) and

Cu,Zn(Aβ)-induced ROS production. This makes possible the use of such water-soluble counterparts for *in vitro* investigations, while the parent ligands could be engaged in *in vivo* experiments.

### 3.2. *Structure–activity relationship*

#### 3.2.1. *Ligands other than $L'_{Me}$*

Ligands other than $L'_{Me}$ are all able to stop Cu(Aβ)-induced ROS production in the absence of Zn(II) when added in the course of Cu(Aβ)-induced Asc. consumption (Experiments "B", Figure 3, first set of columns). Besides, in the presence of increasing ratios of Zn(II) and with long enough incubation times, they all maintain this ability (Figure 3, fourth set of columns, Figures S5 and S7). Finally, when added during the course of Asc consumption, some of them become less and less efficient as the stoichiometry of Zn(II) is increased (Figure 3, second and third sets of columns).

To explain such observations, the chemical reactions shown in Scheme 3 are proposed. According to Scheme 3, the overall Zn(II)-induced slowdown of Cu(II) removal out of Aβ (and consequent effect on Cu(Aβ)-induced Asc consumption) could be due
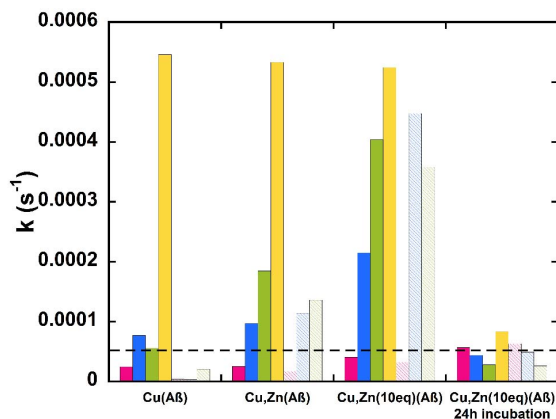
**Figure 3.** Rates of Cu(Aβ)-induced ascorbate consumption as a function of the ligand and equivalent of Zn(II), starting from Cu(I)/Cu(II) (corresponding to data in Figure 2, panels A–C) and from Cu(II) after 24 h of incubation (corresponding to data in Figure 2, panel D and Figure S7). L in pink, $L_{Me}$ in blue, L′ in green, and $L'_{Me}$ in yellow, corresponding sulfonated ligands are displayed in light colors. The rate of Asc consumption was determined by measuring the slope of the Asc consumption curves between the time ($t$) of the addition of $\mathscr{L}$ and $t + 300$ s, approximating the curves as straight lines, and with [Asc] = 100 μM and [Cu] = 10 μM. The dotted line indicates the level of Asc consumption below which Asc consumption is considered to be similar to that of Asc alone in the buffer (due to Asc auto-oxidation).

to both thermodynamic and kinetic factors for each individual reaction at play, the determination of which is beyond the scope of the present study.

Reaction (1) corresponds to Cu(II) removal from Aβ by $\mathscr{L}$ in the absence of Zn(II). Then, in the presence of Zn(II), the addition of $\mathscr{L}$ to Cu,Zn(Aβ) leads to the two possible reactions (2) and (3) and the formation of Cu($\mathscr{L}$) or Zn($\mathscr{L}$), respectively. From a thermodynamic point of view, reaction (2) is much more favored than reaction (3) as probed by the experiments with long incubation times (Experiments "A"). However, reactions (2) and (3) are in kinetic competition, with reaction (3) being faster than reaction (2) because otherwise the presence of Zn(II) would have no strong effect on experiments "B". The progressive loss of the ability to stop Cu(Aβ)-induced
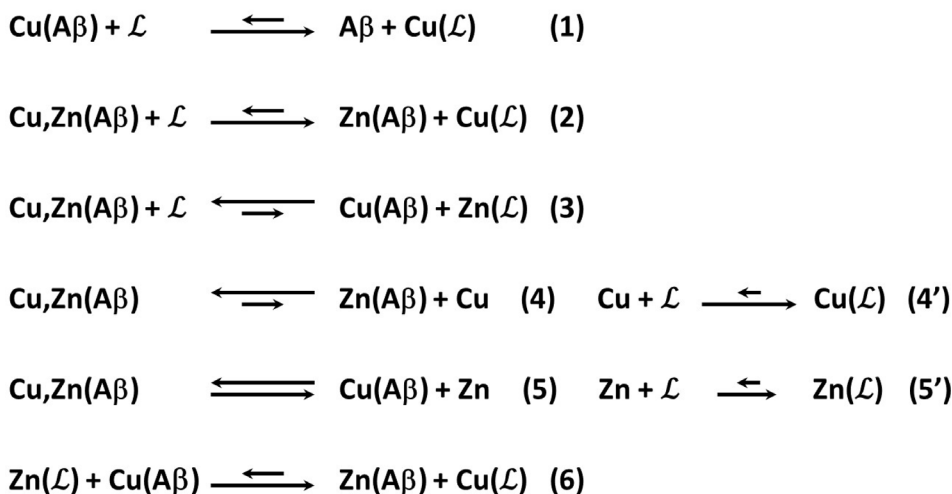
Asc consumption with increasing levels of Zn(II) (Figure 3) thus mirrors the impact of Zn(II) on the overall rate of Cu(II) removal from Aβ. Such an effect may be due (i) to the kinetic competition of Zn(II) with Cu(II) for binding to $\mathscr{L}$ (reaction (2) versus reaction (3)) and/or (ii) to a modification in the rate of reaction (6) (Scheme 3).

With the series of ligands $\mathscr{L}$, Zn(II) induces an overall slowdown of Cu(II) removal. This contrasts with a previous study on peptide-based ligands [44], where an acceleration effect due to Zn-induced Cu expelling from Cu,Zn(Aβ) was reported (corresponding to the path shown by reactions (4) and (4′)). This indicates that reaction (4) is not predominant in the case of $\mathscr{L}$. Hence, it will not be considered in the rest of the discussion.

The best ligands able to resist up to 10 equiv. of Zn are L and $^{s}$L, whereas $^{s}$L′, $L_{Me}$, and $^{s}L_{Me}$ work correctly only in the presence of one equiv. of Zn(II). Hence, the cyclohexyl-grafted ethylene bridge and, to a lesser extent the N-methyl substituents, increase the level of Zn($\mathscr{L}$) versus Cu($\mathscr{L}$) at a given time (before the thermodynamic equilibrium is reached). The weaker effect of L′ on the arrest of Cu(Aβ)-induced Asc consumption may be in line with the reported *cis*-β arrangement (i.e. with the two phenolato moiety being in *cis*) of ligand L′ in $[Cu_2(HL')_2]^{2+}$ species [45] unobserved with other ligands, for which *trans* arrangements (i.e. all the endogenous atoms from $\mathscr{L}$ are in the equatorial plane) were reported [25,46–48]. We can indeed anticipate that such *cis*-β arrangement is more appropriate for Zn(II) versus Cu(II) binding in contrast to the *trans* arrangement which is more appropriate for Cu(II) versus Zn(II).

### 3.2.2. *Ligand $L'_{Me}$*

Among the series, ligand $L'_{Me}$ holds a specific place with very slow kinetics of Cu extraction from Aβ both in the absence (reaction (1)) and presence of Zn(II) (reactions (2)–(6), Scheme 3). In the absence of Zn(II), this is shown in the experiments with a "short" (i.e. 300 s) incubation time (Figure S5, panel A). Indeed, since all the Cu(II) is not extracted from Aβ after such a short time, when Asc is added, its consumption is induced by the remaining Cu(Aβ). To complete the reaction of Cu extraction from Aβ, more than 18 h are required (Figure S6). In the presence of 10 equiv. of Zn(II), this is slightly worse (the

$$Cu(A\beta) + \mathscr{L} \quad \longleftarrow \quad A\beta + Cu(\mathscr{L}) \qquad (1)$$

$$Cu,Zn(A\beta) + \mathscr{L} \quad \longleftarrow \quad Zn(A\beta) + Cu(\mathscr{L}) \quad (2)$$

$$Cu,Zn(A\beta) + \mathscr{L} \quad \longrightarrow \quad Cu(A\beta) + Zn(\mathscr{L}) \quad (3)$$

$$Cu,Zn(A\beta) \quad \longleftarrow \quad Zn(A\beta) + Cu \quad (4) \quad Cu + \mathscr{L} \quad \longleftarrow \quad Cu(\mathscr{L}) \quad (4')$$

$$Cu,Zn(A\beta) \quad \Longleftrightarrow \quad Cu(A\beta) + Zn \quad (5) \quad Zn + \mathscr{L} \quad \longleftarrow \quad Zn(\mathscr{L}) \quad (5')$$

$$Zn(\mathscr{L}) + Cu(A\beta) \quad \longleftarrow \quad Zn(A\beta) + Cu(\mathscr{L}) \quad (6)$$

**Scheme 3.** Various possible reactions at play in Cu(II) removal out of Aβ by $\mathscr{L}$, including in the presence of one equiv. of Zn(II).

level of Asc. consumption lessening in the presence of 10 equiv. of Zn(II) after 24 h equals that in the absence of Zn(II) after 18 h, Figure 2, panel D to be compared with Figure S6). This is due to other reactions coming at play, namely reactions (2)–(6), as described previously for the other ligands. The specific properties of the $L'_{Me}$ ligand may be linked to the combination of the presence of the 1,2-cyclohexyl bridge and the N-methyl group, which makes possible a *cis*-β arrangement of the ligand (i.e. with the two phenolato moiety being in *cis*), described in the solid-state for $Cu(L'_{Me})$ [49]. However this geometry is not recovered in the thermodynamically-stable complex formed in aqueous solution as probed by EPR and to a lesser extent UV–vis signatures. But it may exist transiently and slow down the Cu(II) complex formation (reaction (1)), favor and/or accelerate $Zn(L'_{Me})$ complex formation versus $Cu(L'_{Me})$ complex (reaction (3) versus (2)), and/or disfavor and/or slow down reaction (6) with respect to other ligands in the series. Because the difference between the ability to prevent Cu(Aβ)-induced ROS formation without Zn(II) (Figure S6) and 10 equiv. of Zn(II) (Figure 2D) is fairly weak, we can anticipate that reaction (1) has the most important contribution.

In addition, the trend $L'_{Me} < L' < L_{Me} \ll L$ in the ability to stop Cu(Aβ)-induced ROS formation in the presence of Zn(II) is reminiscent of recently published data using a series of pentadentate lig-

ands ($^{P}$L) based on an ethylene bridge (possibly appended with a cyclo-hexyl moiety: $^{P}$L′, with a N-propyl group: $^{P}$L$_{pro}$ and both: $^{P}$L′$_{pro}$) (Scheme S1). Once chelated with Mn(II), the ligand exchange with Cu(II) that corresponds to reaction (6) here, follows the order: $^{P}$L′$_{pro}$ < $^{P}$L′ < $^{P}$L$_{pro}$ < $^{P}$L (Scheme S2) [28].

### 3.3. *Kinetic impact of Zn(II)*

In brief, the study of the series of ligands $\mathscr{L}$ reveals an impact of Zn(II) on Cu(II) extraction from Aβ that is apparent during the Asc consumption experiments and which is beyond only thermodynamic considerations. Indeed, if Cu,Zn(Aβ) and the ligands are incubated long enough, all the ligands can prevent Cu(Aβ)-induced ROS production. However, in the course of Asc. consumption (no incubation) or when the incubation is short (300 s), ligands $\mathscr{L}$ can be differentiated by their efficiency to stop Cu(Aβ)-induced ROS production in the presence of various Zn(II) levels. Their ability to stop Cu(Aβ)-induced ROS production strongly depends on subtle variations in the ligand scaffold because all the ligands studied here were built on the very same first coordination sphere. Thermodynamic selectivity is now a parameter considered in the design of Cu-targeting ligands in the context of AD [21,22]. In the present study, we also show that it is important to consider the effect of Zn(II) which can modify the rate of Cu(II)

extraction from Aβ by a ligand and can thus prevent the formation of the corresponding Cu(II) complex resistant to Asc. reduction and the associated arrest of Cu(Aβ)-induced ROS production.

### 3.4. *Perspectives*

Among the tested ligands, the simplest L appears to be the ideal candidate with respect to its ability to stop Cu(Aβ)-induced ROS formation in the presence of a biologically relevant ratio of the competing Zn(II) ion. Further studies on this ligand series will aim to relate the *in vitro* data obtained here with their ability to relieve the cellular toxicity induced by ROS produced by Cu(Aβ) with and without Zn, as reported for other ligands [50–54]. Since L is expected to be partly neutral at pH 7 based on potentiometric data reported for $^{G/S}L_{Me}$ [24,25], and thus to fulfill Lipinski's rules, it appears as a good candidate for blood–brain barrier penetration by passive diffusion and thus for further *in vivo* studies on AD animal models.

### Declaration of interests

The authors do not work for, advise, own shares in, or receive funds from any organization that could benefit from this article, and have declared no affiliations other than their research organizations.

### Acknowledgments

### Supplementary data

Supporting information for this article is available on the journal's website under https://doi.org/10.5802/crchim.255 or from the author.

### References

[1] Alzheimer's Association, *Global Dementia Cases Forecasted to Triple by 2050*, 2021, https://aaic.alz.org/releases_2021/global-prevalence.asp.

[2] BrightFocus Foundation, "Alzheimer's Disease: Facts & Figures", 2021, https://www.brightfocus.org/alzheimers/article/alzheimers-disease-facts-figures.

[3] Z. Breijyeh, R. Karaman, *Molecules*, 2020, **25**, article no. 5789.

[4] G. B. Frisoni, D. Altomare, D. R. Thal, F. Ribaldi, R. van der Kant, R. Ossenkoppele, K. Blennow, J. Cummings, C. van Duijn, P. M. Nilsson, P.-Y. Dietrich, P. Scheltens, B. Dubois, *Nat. Rev. Neurosci.*, 2022, **23**, 53-66.

[5] J. Levin, J. Vöglein, Y. T. Quiroz, R. J. Bateman, V. Ghisays, F. Lopera, E. Mcdade, E. Reiman, P. N. Tariot, J. C. Morris, *Alzheimer's Dement.*, 2022, **18**, 2687-2698.

[6] D. J. Selkoe, J. Hardy, *EMBO Mol. Med.*, 2016, **8**, 595-608.

[7] L.-L. Chen, Y.-G. Fan, L.-X. Zhao, Q. Zhang, Z.-Y. Wang, *Bioorg. Chem.*, 2023, **131**, article no. 106301.

[8] C. Hureau, in *Alzheimer's Disease: Recent Findings in Pathophysiology, Diagnostic and Therapeutic Modalities* (T. Govindaraju, ed.), The Royal Society of Chemistry, 2022, 170-192.

[9] T. J. Huat, J. Camats-Perna, E. A. Newcombe, N. Valmas, M. Kitazawa, R. Medeiros, *J. Mol. Biol.*, 2019, **431**, 1843-1868.

[10] M. G. M. Weibull, S. Simonsen, C. R. Oksbjerg, M. K. Tiwari, L. Hemmingsen, *J. Biol. Inorg. Chem.*, 2019, **24**, 1197-1215.

[11] M. Rana, A. K. Sharma, *Metallomics*, 2019, **11**, 64-84.

[12] C. Cheignon, M. Tomas, D. Bonnefont-Rousselot, P. Faller, C. Hureau, F. Collin, *Redox Biol.*, 2018, **14**, 450-464.

[13] S. K. Singh, V. Balendra, A. A. Obaid, J. Esposto, M. A. Tikhonova, N. K. Gautam, B. Poeggeler, *Metallomics*, 2022, **14**, article no. mfac018.

[14] J. Han, Z. Du, M. H. Lim, *Acc. Chem. Res.*, 2021, **54**, 3930-3940.

[15] K. D. Fasae, A. O. Abolaji, T. R. Faloye, A. Y. Odunsi, B. O. Oyetayo, J. I. Enya, J. A. Rotimi, R. O. Akinyemi, A. J. Whitworth, M. Aschner, *J. Trace Elem. Med. Biol.*, 2021, **67**, article no. 126779.

[16] G. Gromadzka, B. Tarnacka, A. Flaga, A. Adamczyk, *Int. J. Mol. Sci.*, 2020, **21**, article no. 9259.

[17] H. W. Ejaz, W. Wang, M. Lang, *Int. J. Mol. Sci.*, 2020, **21**, article no. 7660.

[18] M. G. Savelieff, G. Nam, J. Kang, H. J. Lee, M. Lee, M. H. Lim, *Chem. Rev.*, 2019, **119**, 1221-1322.

[19] Y. Liu, M. Nguyen, A. Robert, B. Meunier, *Acc. Chem. Res.*, 2019, **52**, 2026-2035.

[20] C. Hureau, in *Encyclopedia of Inorganic and Bioinorganic Chemistry* (R. A. Scott, ed.), Wiley, 2019.

[21] C. Esmieu, D. Guettas, A. Conte-Daban, L. Sabater, P. Faller, C. Hureau, *Inorg. Chem.*, 2019, **58**, 13509-13527.

[22] E. Atrian-Blasco, A. Conte-Daban, C. Hureau, *Dalton Trans.*, 2017, **46**, 12750-12759.

[23] A. Conte-Daban, A. Day, P. Faller, C. Hureau, *Dalton Trans.*, 2016, **45**, 15671-15678.

[24] T. Storr, M. Merkel, G. X. Song-Zhao, L. E. Scott, D. E. Green, M. L. Bowen, K. H. Thompson, B. O. Patrick, H. J. Schugar, C. Orvig, *J. Am. Chem. Soc.*, 2007, **129**, 7453-7463.

[25] S. Noël, F. Perez, S. Ladeira, S. Sayen, E. Guillon, E. Gras, C. Hureau, *J. Inorg. Biochem.*, 2012, **117**, 322-325.

[26] T. Kowalik-Jankowska, M. Ruta, K. Wisniewska, L. Lankiewicz, *J. Inorg. Biochem.*, 2003, **95**, 270-282.

[27] S. Noël, S. Bustos, S. Sayen, E. Guillon, P. Faller, C. Hureau, *Metallomics*, 2014, **6**, 1220-1222.

[28] G. Schanne, M. Zoumpoulaki, G. Gazzah, A. Vincent, H. Preud'homme, R. Lobinski, S. Demignot, P. Seksik, N. Delsuc, C. Policar, *Oxid. Med. Cell. Longev.*, 2022, **2022**, article no. 3858122.

[29] E. M. Gale, I. P. Atanasova, F. Blasi, I. Ay, P. Caravan, *J. Am. Chem. Soc.*, 2015, **137**, 15548-15557.

[30] F. K. Kálmán, G. Tircsó, *Inorg. Chem.*, 2012, **51**, 10065-10067.

[31] X. Zhao, D. Zhang, R. Yu, S. Chen, D. Zhao, *Eur. J. Inorg. Chem.*, 2018, **2018**, 1185-1191.

[32] V. J. Lillo, J. Mansilla, J. M. Saá, *Angew. Chem. Int. Ed.*, 2016, **55**, 4312-4316.

[33] I. Correia, J. C. Pessoa, M. T. Duarte, M. F. M. da Piedade, T. Jackush, T. Kiss, M. M. C. A. Castro, C. F. G. C. Geraldes, F. Avecilla, *Eur. J. Inorg. Chem.*, 2005, **2005**, 732-744.

[34] K. Voronova, L. Homolya, A. Udvardy, A. C. Bényei, F. Joó, *ChemSusChem*, 2014, **7**, 2230-2239.

[35] Y. Yong-Kang, Y. Cai-Xia, H. Fang-Jun, *J. Coord. Chem.*, 2014, **67**, 2039-2047.

[36] H. Du, A. H. Velders, P. J. Dijkstra, J. Sun, Z. Zhong, X. Chen, J. Feijen, *Chem. Eur. J.*, 2009, **15**, 9836-9845.

[37] J. Peisach, W. E. Blumberg, *Arch. Biochem. Biophys.*, 1974, **165**, 691-708.

[38] B. Alies, I. Sasaki, O. Proux, S. Sayen, E. Guillon, P. Faller, C. Hureau, *Chem. Commun.*, 2013, **49**, 1214-1216.

[39] E. Atrian-Blasco, E. Cerrada, A. Conte-Daban, D. Testemale, P. Faller, M. Laguna, C. Hureau, *Metallomics*, 2015, **7**, 1229-1232.

[40] A. Conte-Daban, M. Beyler, R. Tripier, C. Hureau, *Chem. Eur. J.*, 2018, **24**, 13058-13058.

[41] A. Conte-Daban, M. Beyler, R. Tripier, C. Hureau, *Chem. Eur. J.*, 2018, **24**, 8447-8452.

[42] K. P. Malikidogo, M. Drommi, E. Atrián-Blasco, J. Hormann, N. Kulak, C. Esmieu, C. Hureau, *Chem. Eur. J.*, 2023, **29**, article no. e202203667.

[43] M. Lefèvre, K. P. Malikidogo, C. Esmieu, C. Hureau, *Molecules*, 2022, **27**, article no. 7903.

[44] P. S. Gonzalez, L. Mathieu, Emilie, P. Faller, C. Hureau, *Biomolecules*, 2022, **12**, article no. 1327.

[45] H. Hosseini-Monfared, S. Soleymani-Babadi, S. Sadighian, A. Pazio, K. Wozniak, M. Siczek, P. Mayer, *Transit. Met. Chem.*, 2015, **40**, 255-267.

[46] P. Adão, S. Barroso, F. Avecilla, M. C. Oliveira, J. C. Pessoa, *J. Organomet. Chem.*, 2014, **760**, 212-223.

[47] A. Hazari, C. Diaz, A. Ghosh, *Polyhedron*, 2018, **142**, 16-24.

[48] Y. Xie, Q. Liu, H. Jiang, J. Ni, *Eur. J. Inorg. Chem.*, 2003, **2003**, 4010-4016.

[49] W. Sun, E. Herdtweck, F. E. Kühn, *New J. Chem.*, 2005, **29**, 1577-1580.

[50] M. Okafor, P. Gonzalez, P. Ronot, I. El Masoudi, A. Boos, S. Ory, S. Chasserot-Golaz, S. Gasman, L. Raibaut, C. Hureau, N. Vitale, P. Faller, *Chem. Sci.*, 2022, **13**, 11829-11840.

[51] S. S. Hindo, A. M. Mancino, J. J. Braymer, Y. Liu, S. Vivekanandan, A. Ramamoorthy, M. H. Lim, *J. Am. Chem. Soc.*, 2009, **131**, 16663-16665.

[52] Y. Yang, T. Chen, S. Zhu, X. Gu, X. Jia, Y. Lu, L. Zhu, *Integr. Biol.*, 2015, **6**, 655-662.

[53] X. Hu, Q. Zhang, W. Wang, Z. Yuan, X. Zhu, B. Chen, X. Chen, *ACS Chem. Neurosci.*, 2016, **7**, 1255-1263.

[54] J.-S. Choi, J. J. Braymer, R. P. R. Nanga, A. Ramamoorthy, M. H. Lim, *Proc. Natl. Acad. Sci. USA*, 2010, **107**, 21990-21995.